

Contents lists available at [ScienceDirect](https://www.sciencedirect.com)

Finance Research Letters

journal homepage: www.elsevier.com/locate/frl

On the information content of implied liquidity measure: Evidence from the S&P 500 index options

Cigdem Yerli ^{a,c}, Zehra Eksi-Altay ^{b,*}, A. Sevtap Selcuk-Kestel ^c^a Bartin Vocational School, Bartin University, Bartin, 74100, Turkiye^b Institute for Statistics and Mathematics, WU-Vienna University of Economics and Business, Welhandelsplatz 1, 1020, Vienna, Austria^c Institute of Applied Mathematics, Middle East Technical University, 06800, Ankara, Turkiye

ARTICLE INFO

Keywords:

Implied liquidity
 Continuous-time Markov chain
 Mean-reversion
 Partial information
 EM algorithm
 Robust filters

ABSTRACT

This paper aims to unfold the information content of the implied liquidity measure, which is introduced through the Conic Finance theory and considered a proxy for the market liquidity level. We propose a partial information setting in which the dynamics of the implied liquidity, representing the noisy information on the unobserved *true market liquidity*, follow a continuous-time Markov-chain modulated exponential Ornstein–Uhlenbeck process. Model inference requires the filtering of the unobserved states of the *true market liquidity*, as well as the estimation of the unknown model parameters. We address the inference problem using the EM algorithm methodology, in which we provide novel results on robust filters leading to maximum likelihood estimates. We fit the proposed model to the implied liquidity series obtained from the prices of (closest to) 1-year ATM call options on the S&P 500 covering the period from January 2002 to August 2022. The data application shows that the unobserved *true market liquidity* follows three regimes. The implied liquidity series contains relevant information as the filtered trajectory of the underlying Markov chain moves according to the economic environment changes due to the Federal Reserve's actions, the global financial crisis of 2007-08, and the COVID-19 pandemic.

1. Introduction

Market liquidity has crucial importance in the smooth functioning of financial markets. The liquidity, or lack thereof, can have a profound impact on the financial system and the overall economy, disrupting their daily operations. Historical events such as the Russian financial crisis in 1998 and the Long-Term Capital Management crash serve as reminders of how even a minor disruption in liquidity can lead to significant and unforeseen consequences. More recently, the financial crisis of 2008 once again highlighted the importance of liquidity in financial markets.

There is no single, universally accepted definition of liquidity; instead, different perspectives and interpretations make measuring market liquidity challenging. Nevertheless, numerous studies have delved into the subject of market liquidity, with earlier works by Kyle (1985), Grossman and Miller (1988), Chordia et al. (2000), and Amihud (2002) shedding light on its significance. Recently, there has been a growing focus on investigating market liquidity through the use of various liquidity measures, as explored by Ramos and Righi (2020), Zaremba et al. (2021) and Christensen and Gillan (2022).

Market liquidity is a multifaceted concept, making it difficult to capture with a single metric (see Kyle, 1985). The bid–ask spread, as a transaction cost-based approach, stands as the most commonly used indicator to evaluate market liquidity levels (see Davis

* Corresponding author.

E-mail addresses: cyerli@bartin.edu.tr (C. Yerli), zehra.eksi@wu.ac.at (Z. Eksi-Altay), skestel@metu.edu.tr (A.S. Kestel).<https://doi.org/10.1016/j.frl.2023.104164>

Received 5 May 2023; Received in revised form 21 June 2023; Accepted 28 June 2023

Available online 1 July 2023

1544-6123/© 2023 The Authors. Published by Elsevier Inc. This is an open access article under the CC BY license (<http://creativecommons.org/licenses/by/4.0/>).

et al., 1993; Shreve and Soner, 1994; Cvitanic and Karatzas, 1996; and Barles and Soner, 1998). However, many models based on bid–ask spreads fail to account for the observed spread magnitudes in financial markets fully. This deficiency became particularly evident after the 2008 financial crisis, during which bid–ask spreads for many assets remained consistently high, surpassing what could be explained solely by transaction costs. Additionally, bid–ask spreads can fluctuate in response to volatility or changes in the spot price of an asset, irrespective of any actual changes in the underlying asset’s liquidity. To address this issue, Corcuera et al. (2012) introduces the *implied liquidity* measure that facilitates liquidity comparisons across different assets and markets. Albrecher et al. (2013) further expanded on this concept by fitting various stochastic models to the implied liquidity time series, suggesting a stochastic, regime-switching, mean-reverting process as a suitable approach.

In this paper, we propose a setting to analyze the information content of the implied liquidity measure as a proxy for the unobservable *true market liquidity* level. Recognizing the unobservability aspect of liquidity, we work in a partial-information setting where the implied liquidity measure is considered a noisy indicator of the unobserved *true market liquidity*. Naturally, the *true market liquidity* level is subject to policy changes, such as shifts from quantitative easing to tightening or transitions between bullish and bearish market conditions. To capture this dynamic nature, we model the *true market liquidity* level as a continuous-time finite-state Markov chain. Additionally, drawing upon previous findings that suggest a regime-switching mean-reverting process as an appropriate liquidity model (see Albrecher et al., 2013), we fit a Markov-chain modulated exponential Ornstein–Uhlenbeck (OU) process to the *implied liquidity* series derived from prices of (closest to) 1-year ATM call options on the S&P 500 index.

Hidden Markov models (HMM) have been widely employed in other studies to analyze market liquidity regimes. For example, Flood et al. (2015) use a discrete-time HMM to examine system-wide liquidity conditions across various asset classes, concluding that three regimes adequately capture the dynamics. Tenyakov et al. (2016) investigate the relationship between funding and market liquidity using a hidden Markov-modulated OU model, finding that a 2-state model adequately explains the relationship. Similarly, Gu et al. (2021) propose a hybrid multivariate discrete-time hidden Markov-modulated OU and geometric Brownian motion models to capture regime switches and demonstrate the sufficiency of two regimes in explaining the dynamics.

We use the Expectation-Maximization (EM) algorithm methodology to address the model inference problem. The work by Elliott et al. (1999) provides the filtering and parameter estimation results for the Markov-chain modulated OU process. However, our novel contribution lies in providing an EM algorithm methodology with *robust* filtering and discretization in the sense of James et al. (1996). By incorporating robust filters, we effectively mitigate numerical issues that may arise in applications with discrete observations. Additionally, this approach allows us to estimate the unknown noise variance within the algorithm.

Applying our proposed model to options data shows that the unobserved *true market liquidity* exhibits three distinct regimes. Furthermore, the *implied liquidity* series contains valuable information that reflects market liquidity variations stemming from factors such as Federal Reserve (Fed) interventions, financial crises, and the COVID-19 pandemic. Consequently, this paper contributes to the understanding of market liquidity dynamics by introducing a model that effectively captures the relationship between the *implied liquidity* measure and the underlying *true market liquidity*. Such insights offer decision-makers in policy and practice a framework for effectively managing market liquidity.

The remaining sections of this paper are structured as follows: Section 2 introduces the model setting, while Section 3 presents the results of robust filtering and the EM algorithm. In Section 4, we provide details about the data used in our study, present and discuss the application results. The appendix includes the proof of the main proposition.

2. Underlying model setting

We consider a finite time interval $[0, T]$ and a filtered probability space $(\Omega, \mathcal{F}, \mathbb{F}, \mathbb{P})$, where $\mathbb{F} = (\mathcal{F}_t)_{t \geq 0}$ is the global filtration that satisfies the usual conditions.

We assume a Black–Scholes setting with an underlying asset S with volatility σ and the risk-free interest rate $r > 0$. We recall that, under the Conic Finance theory with a Wang distortion function and implied liquidity L , the bid price of a European call option written on S , with the strike price K and the maturity T is given as (see, e.g., Guillaume et al., 2019, Eqs. 15–16):

$$b_{L,t} = S_t \exp(-L\sigma\sqrt{T-t})\mathcal{N}(d_1 - L) - K \exp(-r(T-t))\mathcal{N}(d_2 - L), \quad (1)$$

where $d_1 = \frac{\ln(S_t/K) + (r + \sigma^2/2)(T-t)}{\sigma\sqrt{T-t}}$, $d_2 = d_1 - \sigma\sqrt{T-t}$, and \mathcal{N} indicates the standard Normal distribution function. The ask price of the option is:

$$a_{L,t} = S_t \exp(L\sigma\sqrt{T-t})\mathcal{N}(d_1 + L) - K \exp(-r(T-t))\mathcal{N}(d_2 + L), \quad (2)$$

where $d_1 = \frac{\ln(S_t/K) - (r + \sigma^2/2)(T-t)}{\sigma\sqrt{T-t}}$, $d_2 = d_1 - \sigma\sqrt{T-t}$.

Naturally, the *true market liquidity* level is prone to policy changes, for example, from quantitative easing to tightening or financial market regime shifts from bullish to bearish market conditions. Accordingly, we model the true market liquidity level with a continuous-time finite-state Markov chain $X = \{X_t; 0 \leq t \leq T\}$ with the state space $S = \{e_1, e_2, \dots, e_K\}$, where e_k is the k th basis column vector of \mathbb{R}^K . We assume a given initial probability distribution π_0 , and the transpose of the infinitesimal generator of X is denoted by A . Thus, $A = (a^{ij})$ such that, for $i \neq j$, $a^{ij} \geq 0$, $a^{ij} = -\sum_{i \neq j} a^{ij}$, $i, j \in \{1, \dots, K\}$.

We consider *implied liquidity* series to provide noisy information on the *true market liquidity* level. Brunnermeier and Pedersen (2009) and Brunnermeier (2009) report the “self-stabilizing behavior” of market liquidity, which may manifest itself in implied liquidity series having mean-reversion property. Corcuera et al. (2012) support the idea of mean-reverting behavior, which is also

confirmed by Albrecher et al. (2013). Putting those properties together with the positivity of the implied liquidity measure, we model the *logarithm of implied liquidity* as a Markov-chain modulated OU process:

$$dY_t = \kappa(\bar{g}(X_t) - Y_t)dt + \zeta W_t, \tag{3}$$

where $\kappa > 0$ is the mean reversion speed, $\bar{g}(X_t)$ is the regime switching mean-reversion level, ζ is the diffusion coefficient, and W , representing the noise, is a standard (\mathbb{F}, \mathbb{P}) -Brownian motion independent of X . Here we point out that the regime changes on true market liquidity impact the long-run *equilibrium level* of implied liquidity.

We denote by L the *implied liquidity*. Applying Ito's formula to $L_t = \exp(Y_t)$ yields the following dynamics (note that variant of this model (without Markov-chain modulation) is also known as Schwartz reduced-form model (Schwartz, 1997)):

$$dL_t = \kappa(\bar{g}(X_t) + \frac{\zeta^2}{2} - \log(L_t))L_t dt + \zeta L_t dW_t. \tag{4}$$

We assume that the Markov chain X representing the *true market liquidity* level is not directly observable, and the market participants observe only the implied liquidity. In (3), $\zeta > 0$ determines the magnitude of noise in the continuous noisy observations of X .

The information accessible to the observer of system is carried in the sigma algebra generated by the filtration \mathbb{Y} , that is

$$\mathbb{Y} = (\mathcal{Y}_t)_{t \geq 0}, \quad \mathcal{Y}_t = \sigma\{L_s, 0 \leq s \leq t\} = \sigma\{Y_s, 0 \leq s \leq t\}.$$

Accordingly, we consider the full information filtration \mathbb{F} as the augmented filtration containing information on the Markov chain and the implied liquidity:

$$\mathbb{F} = (\mathcal{F}_t)_{t \geq 0}, \quad \mathcal{F}_t = \sigma\{L_s, X_s, 0 \leq s \leq t\} = \sigma\{Y_s, X_s, 0 \leq s \leq t\}.$$

We define the *normalized observation* process $y_t = Y_t/\zeta$. Denote by $g = \bar{g}(\cdot)/\zeta$, we have:

$$dy_t = \kappa(g(X_t) - y_t)dt + W_t. \tag{5}$$

Hence, during the theoretical analysis, one may assume without loss of generality that $\zeta = 1$. In theory, the value of ζ is equal to $[Y]_t/t$ where $[Y]$ is the quadratic variation of Y and is thus observable. However, in practice, the observations are not continuous, and ζ has to be estimated. This problem is addressed in Section 3.

3. EM methodology and filtering

Regarding model estimation, the partial information setting prevents us from using standard tools such as MLE. Instead, one can address the inference problem using the Expectation-Maximization (EM) algorithm methodology. Elliott et al. (1999) introduce the filtering and parameter estimation for the Markov-chain modulated OU process. In the following, we extend the existing results by providing an EM algorithm methodology with robust filtering and discretization in the sense of James et al. (1996).

For an integrable and measurable process Z , the \mathbb{Y} -optional projection $\hat{Z}_t := E[Z_t | \mathcal{Y}_t]$ a.s. for all $t \leq T$, gives the filtered estimate of Z_t . For a generic function f , it holds that $f(X_t) = \langle X_t, \mathbf{f} \rangle$ where $\langle \cdot, \cdot \rangle$ denotes the scalar product and $\mathbf{f}_k = f(e_k)$, $1 \leq k \leq K$ so that functions of the Markov chain can be identified with K -vectors. Hence, it follows that the unobserved parameters to be estimated are given by the vector $\theta = (a^{ij}, g^j, \kappa, \zeta; i, j \in \{1, \dots, K\})$.

Our goal is to utilize the EM methodology to estimate the model parameters and infer the unobserved realizations of the state process X , given the observations Y_t , $0 \leq t \leq T$. Denote by \mathbb{P}_θ the probability measures corresponding to the parameter vector θ . Due to the unobservability of the Markov chain X , it is not possible to determine the full-information likelihood function. In the current setting, we have the following *partial-information log-likelihood ratio* (see, e.g., Elliott et al., 1999):

$$\widehat{L}(\theta, \theta') := \log \frac{d\mathbb{P}_\theta}{d\mathbb{P}_{\theta'}} \Big|_{\mathcal{Y}_T} = \sum_{i=1}^N (\kappa g^i \hat{G}_T^i - \frac{1}{2} \kappa g^{i^2} \hat{J}_T^i + \kappa g^i \hat{I}_T^i) + \sum_{\substack{i \neq j \\ i, j=1}}^N (\hat{N}_T^{ij} \log(a^{ij}) - a^{ij} \hat{J}_T^i) + \hat{R}(\theta'), \tag{6}$$

where $\hat{R}(\theta')$ is independent of θ , and we have: J_t^i is the sojourn time of the Markov chain in state i until time t ; N_t^{ij} is the number of transitions from state i to j of the process X where $i \neq j$ up to time t ; G_t^i is the level sum of the integral for state e_i until time t ; I_t^i is the time t value of an auxiliary process for the state i .

The EM algorithm is an iterative procedure that leads to a sequence θ^m of parameter estimates such that the likelihood of the observations increases in each step. Given the optimal parameter vector θ^m after the m th iteration of the algorithm, the $(m + 1)^{th}$ iteration of the EM algorithm consists of the following two steps:

- i. **Expectation (E):** Compute the filtered estimate of the partial information log-likelihood $\widehat{L}(\theta, \theta^m)$.
- ii. **Maximization (M):** Find $\theta^{m+1} \in \underset{\theta}{\operatorname{argmax}} \widehat{L}(\theta, \theta^m)$.

Since $\widehat{L}(\cdot, \theta^m)$ is concave, the new parameter vector θ^{m+1} is given by equating the partial derivatives of (6) to zero. We thus obtain that

$$(a^{ij})^{m+1} = \frac{\hat{N}_T^{ij}}{\hat{J}_T^i}, \quad (g^j)^{m+1} = \frac{(\kappa^{m+1})^{-1} \hat{G}_T^j + \hat{I}_T^j}{\hat{J}_T^i}, \quad (\kappa)^{m+1} = \frac{C}{D}, \tag{7}$$

where, $C = \int_0^T y_s dy_s - \sum_{i=1}^N \frac{\hat{I}_T^i \hat{G}_T^i}{\hat{J}_T^i}$ and $D = \sum_{i=1}^N \frac{(\hat{I}_T^i)^2}{\hat{J}_T^i} - \int_0^T y_s^2 dy_s$.

It is evident in (7) that one has to obtain the filtered estimates of the quantities in (6) to determine the optimal parameters. This is a non-linear filtering problem, and the corresponding theoretical results on normalized and unnormalized filters, denoted by $\bar{\sigma}(\cdot)$ and $\sigma(\cdot)$, respectively, can be found, e.g., in Elliott et al. (1999). Note that expressions for the optimal parameters can also be obtained by replacing normalized filters with unnormalized versions.

In most finance applications, the data constitute discrete observations. No matter the frequency of data observations, one must discretize the (continuous) filtering results. Applying standard discretization techniques (such as Euler–Maruyama) to normalized or unnormalized filters may result in numerical issues and the non-smoothness of the filtered state trajectories. Thus, in Proposition 3.1, we obtain the so-called robust filters in the sense of James et al. (1996). Here, the idea is to transform the filter dynamics so that the resulting expressions involve minimal stochastic integrals. The derivation of robust filters requires the unnormalized filters $\sigma(H_T)$ for $H_T = N_T^{ij}, G_T^i, J_T^i$ and I_T^i and $\sigma(H_T) = \langle \sigma(H_T X_T), \mathbf{1} \rangle$ where $\mathbf{1} = \text{diag}(1, \dots, 1)$.

Proposition 3.1 (Robust Filters). Let Φ given by $\Phi_t = \exp(\kappa B_t y_t - \frac{1}{2} \kappa^2 B_t^2 t)$ and let Φ_t^{-1} denote its inverse. The unnormalized filter $\sigma(X_t)$ of the state process X has a robust version defined as

$$\bar{\sigma}(X_t) = \Phi_t^{-1} \sigma(X_t), \quad \bar{\sigma}(X_0) = \sigma(X_0),$$

which is a finite variation process and solves the linear ordinary differential equation (ODE) in \mathbb{R}^K :

$$\frac{d}{dt} \bar{\sigma}(X_t) = \Phi_t^{-1} A \Phi_t \bar{\sigma}(X_t), \quad \bar{\sigma}(X_0) = \sigma(X_0). \tag{8}$$

Moreover, we have

$$\begin{aligned} d\bar{\sigma}(N_t^{ij} X_t) &= \langle \bar{\sigma}(X_t), e_i \rangle \alpha^{ij} e_j dt + \Phi_t^{-1} A \Phi_t \bar{\sigma}(N_t^{ij} X_t) dt, \quad \bar{\sigma}(N_0^{ij} X_0) = 0, \\ d\bar{\sigma}(J_t^i X_t) &= \langle \bar{\sigma}(X_t), e_i \rangle e_i dt + \Phi_t^{-1} A \Phi_t \bar{\sigma}(J_t^i X_t) dt, \quad \bar{\sigma}(J_0^i X_0) = 0, \\ d\bar{\sigma}(G_t^i X_t) &= \langle \bar{\sigma}(X_t), e_i \rangle e_i dy_t + \Phi_t^{-1} A \Phi_t \bar{\sigma}(G_t^i X_t) dt, \quad \bar{\sigma}(G_0^i X_0) = 0, \\ d\bar{\sigma}(I_t^i X_t) &= y_t \langle \bar{\sigma}(X_t), e_i \rangle e_i dt + \Phi_t^{-1} A \Phi_t \bar{\sigma}(I_t^i X_t) dt, \quad \bar{\sigma}(I_0^i X_0) = 0. \end{aligned}$$

Proof. Proof is provided in Appendix.

After obtaining the robust filters, we follow the methodology given in James et al. (1996) and discretize the robust filters by Euler–Maruyama method. That yields an equivalent discrete time model: for a small enough time step $\Delta = t_n - t_{n-1}$, $P^* = [I + \Delta A]$ represents transition probabilities of the corresponding discrete time Markov chain X_n ; the discrete time observations are represented through the fast-sampled observations $z_n^\Delta = (y_n - y_{n-1})/\Delta$, $n = 1, 2, \dots, N$. Then we set, e.g., $\sigma(X_n) = \Phi_{t_n} \bar{\sigma}(X_n)$, and let $\Psi_n = \Phi_{t_n} \Phi_{t_{n-1}}^{-1}$. We define the normalization constant $c_n = \langle \Psi_n P^* \sigma(X_{n-1}), \mathbf{1} \rangle$ and obtain the following normalized discrete time recursive filters:

$$\begin{aligned} \sigma(X_n) &= \Psi_n P^* \sigma(X_{n-1}) / c_n, \\ \sigma(N_n^{ij} X_n) &= [\Psi_n P^* \sigma(N_{n-1}^{ij} X_{n-1}) + \langle \sigma(X_{n-1}), e_i \rangle \langle \Psi_n P^* e_i, e_j \rangle] / c_n, \\ \sigma(J_n^i X_n) &= [\Psi_n P^* \sigma(J_{n-1}^i X_{n-1}) + \langle \sigma(X_{n-1}), e_i \rangle \Psi_n P^* e_i] / c_n, \\ \sigma(G_n^i X_n) &= [\Psi_n P^* \sigma(G_{n-1}^i X_{n-1}) + z_n^\Delta \langle \sigma(X_{n-1}), e_i \rangle \Psi_n P^* e_i] / c_n, \\ \sigma(I_n^i X_n) &= [\Psi_n P^* \sigma(I_{n-1}^i X_{n-1}) + y_{n-1} \langle \sigma(X_{n-1}), e_i \rangle \Psi_n P^* e_i] / c_n. \end{aligned}$$

Under the discretized setting, following the methodology in Section VI of James et al. (1996), we obtain the ML estimate of the unknown noise variance:

$$\hat{\varsigma}^2 = -\frac{\Delta}{N} \left(\sum_{i=1}^K (\kappa^2 (g^i)^2 (\hat{J}_N^i)^2 - 2\kappa^2 g^i \hat{I}_N^i - 2\kappa g^i \hat{G}_N^i) + \sum_{n=1}^N |z_n^\Delta|^2 + \kappa^2 |y_{n-1}|^2 + 2\kappa |y_{n-1} z_n^\Delta| \right).$$

4. Application to S&P 500 index options

This section implements the model on the S&P 500 index options data. We use the S&P 500 index options data due to several reasons. Given its size, scope, and influence on other markets, the S&P 500 index is considered a key proxy for the U.S. economy. Thus, the index options data may also represent the overall stock options market well. Moreover, the composition of the S&P 500 index allows us to assume that the company-related (idiosyncratic) effects on the calculation of option values will be minor and that any significant changes in option prices can be attributed to financial market factors.

4.1. The data

The data comprise the daily bid and ask prices of European call options written on the S&P 500 index from January 2002 to August 2022.¹ The data set also contains daily values of the underlying S&P 500 index, daily values of the implied volatility, and daily values of the 3-month US Treasury bill rate.²

A large data set with 34,438,878 price observations with various strikes and maturities are employed. We produce the implied liquidity series following the procedure in Albrecher et al. (2013). Denote by n the n th day of the data period $n \in 1, \dots, N$. On each day of the sample period, we first choose an option based on two criteria: (closest to) 1-year ATM call options and the highest trading volume if several options are available the same day after applying the first criteria. After extracting the option series, we find the implied liquidity parameter, L_n , that best matches the theoretical bid–ask prices with the observed bid–ask prices at day n : we obtain the implied liquidity by minimizing the squared error (SE) between the theoretical bid–ask prices ($a_{L,n}$, $b_{L,n}$) and the observed bid–ask prices (a_n , b_n). That is, we solve the following minimization problem:

$$\begin{aligned} \min_{L_n} \quad & SE_{bid,ask}(L_n) = ((b_n - b_{L,n})^2 + (a_n - a_{L,n})^2) \\ \text{s.t.} \quad & L_n \geq 0. \end{aligned}$$

We repeat this procedure each day of the data and obtain the implied liquidity series. Then, we multiply the resulting series with 100 to obtain the values in basis points.

4.2. Implementation, results and discussion

As next, we fit the proposed model to the implied liquidity series. As it is not a priori clear how many states one should assume for the underlying Markov chain, we refer to the related literature (see, e.g., Flood et al., 2015) and set the number of states $K = 3$, representing the three liquidity regimes: low, intermediate, and high. We apply the EM algorithm with the following steps:

Step 1: Initialize the algorithm with parameters θ^0 .

Step 2: Obtain the robust filtered estimates of the quantities of interest.

Step 3: Compute θ^{n+1} .

Step 4: Terminate if $\frac{|\theta^{n+1} - \theta^n|}{|\theta^n|}$ are below the termination tolerance 0.01; else return to step N.

The evolution and convergence of parameter estimates are depicted in Fig. 1, indicating that the algorithm is relatively fast, converging on iteration 15. The estimated generator matrix with respect to *Low* (state 1), *Intermediate* (state 2) and *High* (state 3) states is presented in Table 1 at which the estimated intensities of transitions from *High* to *Low* and *Low* to *High* states are zero. The parameter estimates for the observation process are presented in Table 2. Moreover, the corresponding log-likelihood (LL) and the Mean Absolute Percentage Error (MAPE) values are computed as $LL = 109.912$, $MAPE = 1.5859e - 05$. The high value of the log-likelihood and minimal value of the MAPE indicate a good performance of the model.³

We depict the logarithm of the daily implied liquidity series on the upper panel of Fig. 2. By definition, higher value of implied liquidity corresponds to lower liquidity level in the underlying market and vice versa. We also provide the filtered trajectory of the Markov chain, representing the unknown true market liquidity level, in the lower panel of Fig. 2. It is natural to expect that any sound measure of market liquidity should reflect the changes in market liquidity due to changes in the underlying economic environment. The market liquidity level in the U.S. has been influenced by various factors, including the Fed's monetary policy, economic conditions, and global events. The Fed started cutting interest rates in 2002 to stimulate the economy following the 2001 recession. The implied liquidity measure captures this increase in liquidity (see region P1 in Fig. 2). By 2005, inflation was becoming a concern, and the Fed began raising interest rates to keep it under control. The housing market was experiencing a bubble at this time due to increased sub-prime mortgages. The use of complex financial instruments and leverage was on the rise, which would eventually lead to the global financial crisis of 2007–08 (see Helleiner, 2011; Gorton, 2012; and Brunnermeier, 2009). All these reasons led to a decrease in the market liquidity level starting from 2005, and it experienced its lowest level between mid-2005 and mid-2009. The financial crisis erupted in 2007 and continued to escalate, and in response, central banks worldwide, including the Fed, took several interventions. The money injections increased the liquidity level slightly in 2008 but were not enough to prevent the financial crisis. While the liquidity shortage during the mid-2005 and mid-2009 could not immediately be reflected in the S&P 500 index itself, it is present in the filtered trajectory of the unobservable *true market liquidity* (see region P2 in Fig. 2).

In response to the 2008 financial crisis, the Fed implemented a series of large-scale asset purchases known as quantitative easing (QE). In 2013, the Fed declared its intention to gradually decrease its asset purchases and reduce monthly bond purchases, ultimately concluding the QE program in 2015. Nevertheless, between the end of 2013 and the start of 2014, the market experienced a period of high liquidity due to the three QE programs implemented. That increase in liquidity manifests as an increase in the filtered trajectory of the Markov chain over the region P3. Within the period covering 2014 to 2018, the Fed kept the size of its balance

¹ The data is obtained from ivolatility.com

² Interest rate data is obtained from fred.stlouis.org

³ We also fit a 2-state Markov-chain model, which performs worse than the current one whose results can be provided upon request.

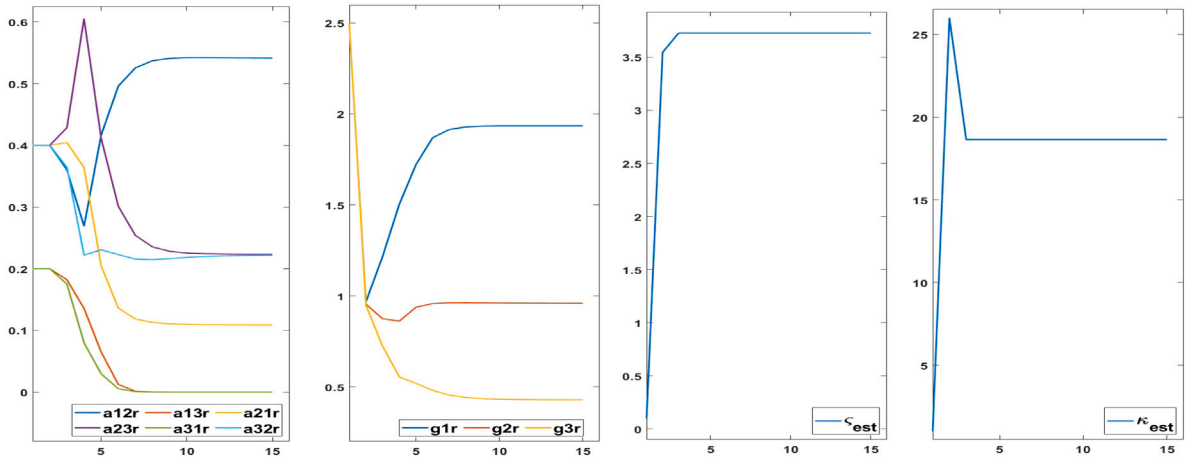


Fig. 1. Evolution of parameter estimates during the iterations of EM algorithm (left to right: \hat{a} , \hat{g} , $\hat{\zeta}$, $\hat{\kappa}$).

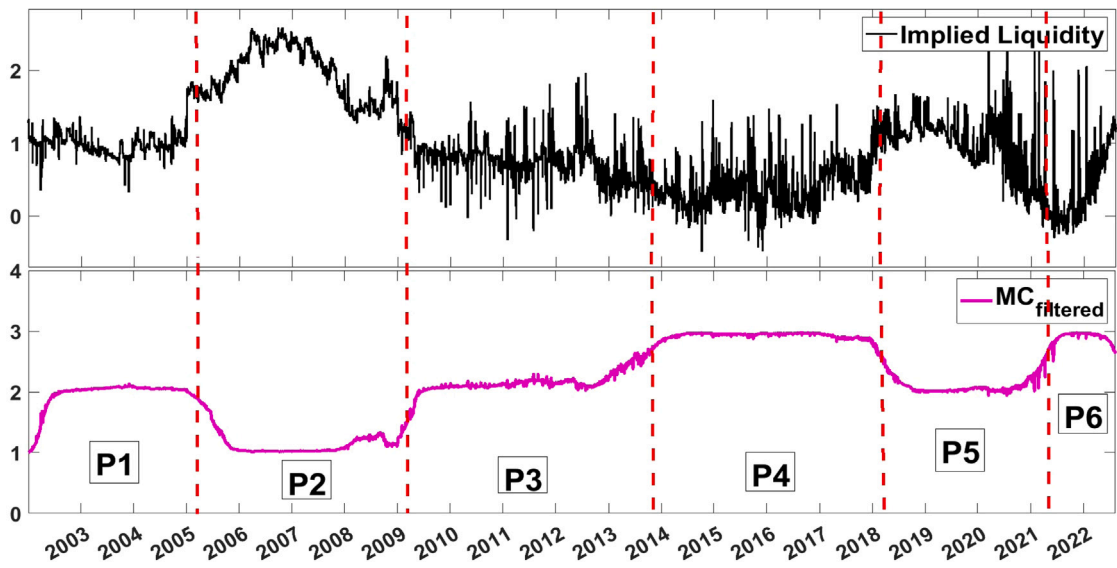


Fig. 2. Implied liquidity series and filtered estimate of the Markov-chain trajectory: Logarithm of implied liquidity (top) and filtered states of X (bottom).

Table 1
Estimated generator matrix of the Markov chain X with three states.

	Low	Intermediate	High
Low	-0.542	0.542	0.000
Intermediate	0.109	-0.331	0.222
High	0.000	0.222	-0.222

Table 2
Parameter estimates for the observation process: g , κ and ζ .

\hat{g}_{low}	$\hat{g}_{intermediate}$	\hat{g}_{high}	$\hat{\kappa}$	$\hat{\zeta}$
1.934	0.959	0.428	18.658	3.804

sheet steady; thus, tapering program had a limited effect on the market liquidity. A high market liquidity level characterized the period between 2014 and 2018, again reflected in the filtered trajectory in the region **P4**.

Throughout 2017–2018, the Fed raised interest rates several times. It reduced the size of its balance sheet through gradual asset runoff, which led to a decrease in the market liquidity level as reflected by the behavior of implied liquidity series in the region **P5** of Fig. 2. However, in response to the economic challenges posed by the COVID-19 pandemic, the Fed paused its interest rate hikes and began to expand its balance sheet again, which led to again high market liquidity level (see Chari et al., 2021) as seen in the region **P6**.

In summary, our findings demonstrate the strong association between the filtered trajectory of the underlying Markov chain and significant economic events, including the actions of the Fed, the global financial crisis of 2007–08, and the COVID-19 pandemic. This highlights the immense value of the implied liquidity series as a reliable indicator of market liquidity level and its fluctuations over time. The ability to accurately assess the true state of market liquidity empowers decision-makers to make informed interventions and take proactive measures to prevent liquidity shortages or crises. By closely monitoring and analyzing the implied liquidity series, policymakers can adjust their strategies in response to changes in economic conditions and the actions of central banks. Moreover, market participants can utilize this information to make more informed investment decisions, optimize trading strategies, and effectively manage their exposure to liquidity risks.

Declaration of competing interest

The authors declare the following financial interests/personal relationships which may be considered as potential competing interests: Cigdem Yerli reports financial support was provided by TUBITAK.

Data availability

The authors do not have permission to share data.

Acknowledgments

The work on this paper was completed while Cigdem Yerli was visiting the Institute for Statistics and Mathematics, WU Vienna. The author greatly acknowledges the funding from the TUBITAK (Turkish Scientific and Technical Research Council) under grant 1059B142100332.

Appendix

Proof. Proof of Proposition 3.1

Given the dynamics of unnormalized filter $\sigma(X_t)$ in Elliott et al. (1999), we apply Ito's product rule to $\Phi_t^{-1}\sigma(X_t)$.

$$\begin{aligned} d\bar{\sigma}(X_t) &= d\Phi_t^{-1}\sigma(X_t) \\ &= \Phi_t^{-1}d\sigma(X_t) + d\Phi_t^{-1}\sigma(X_t) + [\Phi_t^{-1}, \sigma(X)]_t \\ &= \Phi_t^{-1}A\sigma(X_t)dt + \kappa B_t\Phi_t^{-1}\sigma(X_t)dy_t - \kappa B_t\Phi_t^{-1}\sigma(X_t)dy_t \\ &\quad + \kappa^2 B_t^2\Phi_t^{-1}\sigma(X_t)dt - \kappa^2 B_t^2\Phi_t^{-1}\sigma(X_t)dt \\ &= \Phi_t^{-1}A\sigma(X_t), \end{aligned}$$

with replacing $\sigma(X_t) = \Phi_t\bar{\sigma}(X_t)$,

$$\bar{\sigma}(X_t) = \Phi_t^{-1}A\Phi_t\bar{\sigma}(X_t)dt.$$

In the same vein, applying Ito's product formula to $\Phi_t^{-1}\sigma(N_t^{ij}X_t)$, $\Phi_t^{-1}\sigma(J_t^iX_t)$, $\Phi_t^{-1}\sigma(G_t^iX_t)$ and $\Phi_t^{-1}\sigma(I_t^iX_t)$ gives the corresponding robust filters.

References

- Albrecher, H., Guillaume, F., Schoutens, W., 2013. Implied liquidity: Model sensitivity. *J. Empir. Financ.* 23, 48–67.
- Amihud, Y., 2002. Illiquidity and stock returns: cross-section and time-series effects. *J. Financial Mark.* 5 (1), 31–56.
- Barles, G., Soner, H.M., 1998. Option pricing with transaction costs and a nonlinear black-scholes equation. *Finance Stoch.* 2 (4), 369–397.
- Brunnermeier, M.K., 2009. Deciphering the liquidity and credit crunch 2007–2008. *J. Econ. Perspect.* 23 (1), 77–100.
- Brunnermeier, M.K., Pedersen, L.H., 2009. Market liquidity and funding liquidity. *Rev. Financ. Stud.* 22 (6), 2201–2238.
- Chari, A., Dilts Stedman, K., Lundblad, C., 2021. Taper tantrums: Quantitative easing, its aftermath, and emerging market capital flows. *Rev. Financ. Stud.* 34 (3), 1445–1508.
- Chordia, T., Roll, R., Subrahmanyam, A., 2000. Commonality in liquidity. *J. Financ. Econ.* 56 (1), 3–28.
- Christensen, J.H., Gillan, J.M., 2022. Does quantitative easing affect market liquidity? *J. Bank. Financ.* 134, 106349.
- Corcuera, J.M., Guillaume, F., Madan, D.B., Schoutens, W., 2012. Implied liquidity: towards stochastic liquidity modelling and liquidity trading. *Int. J. Portfolio Anal. Manag.* 1 (1), 80–91.
- Cvitanic, J., Karatzas, I., 1996. Hedging and portfolio optimization under transaction costs: A martingale approach. *Math. Finance* 6 (2), 133–165.

- Davis, M.H., Panas, V.G., Zariphopoulou, T., 1993. European option pricing with transaction costs. *SIAM J. Control Optim.* 31 (2), 470–493.
- Elliott, R.J., Fischer, P., Platen, E., 1999. Filtering and parameter estimation for a mean reverting interest rate model. *Can. Appl. Math. Q.* 7 (4), 381–400.
- Flood, M.D., Liechty, J., Piontek, T., 2015. Systemwide commonalities in market liquidity. Available at SSRN 2612348.
- Gorton, G., 2012. *Misunderstanding Financial Crises: Why We Don't See Them Coming*. Oxford University Press.
- Grossman, S.J., Miller, M.H., 1988. Liquidity and market structure. *J. Finance* 43 (3), 617–633.
- Gu, X., Mamon, R., Davison, M., Yu, H., 2021. An automated financial indices-processing scheme for classifying market liquidity regimes. *Internat. J. Control* 94 (3), 735–756.
- Guillaume, F., Junike, G., Leoni, P., Schoutens, W., 2019. Implied liquidity risk premia in option markets. *Ann. Finan.* 15, 233–246.
- Helleiner, E., 2011. Understanding the 2007–2008 global financial crisis: Lessons for scholars of international political economy. *Annu. Rev. Political Sci.* 14, 67–87.
- James, M.R., Krishnamurthy, V., Le Gland, F., 1996. Time discretization of continuous-time filters and smoothers for HMM parameter estimation. *IEEE Trans. Inform. Theory* 42 (2), 593–605.
- Kyle, A.S., 1985. Continuous auctions and insider trading. *Econometrica* 53, 1315–1335.
- Ramos, H.P., Righi, M.B., 2020. Liquidity, implied volatility and tail risk: A comparison of liquidity measures. *Int. Rev. Financ. Anal.* 69, 101463.
- Schwartz, E.S., 1997. The stochastic behavior of commodity prices: Implications for valuation and hedging. *J. Finance* 52 (3), 923–973.
- Shreve, S.E., Soner, H.M., 1994. Optimal investment and consumption with transaction costs. *Ann. Appl. Probab.* 4 (3), 609–692.
- Tenyakov, A., Mamon, R., Davison, M., 2016. Filtering of a discrete-time HMM-driven multivariate Ornstein-Uhlenbeck model with application to forecasting market liquidity regimes. *IEEE J. Sel. Top. Sign. Proces.* 10 (6), 994–1005.
- Zaremba, A., Aharon, D.Y., Demir, E., Kizys, R., Zawadka, D., 2021. COVID-19, government policy responses, and stock market liquidity around the world: A note. *Res. Int. Bus. Finance* 56, 101359.